Journal of Geophysical Research: Atmospheres

RESEARCH ARTICLE
10.1029/2018JD028622

Key Points:
- Methane and ethane emissions are quantified from five separate oil- and gas-producing regions in the central/western United States
- The atmospheric enhancement of ethane to methane downwind of these regions is similar to their abundance in locally produced natural gas
- This study provides the first basin-wide emission estimates from the Eagle Ford shale region in Texas using airborne data

Supporting Information:
- Supporting Information S1

Correspondence to:
J. Peischl,
jeff.peischl@noaa.gov

Citation:
Peischl, J., Eilerman, S. J., Neuman, J. A., Aikin, K. C., de Gouw, J., Gilman, J. B., et al. (2018). Quantifying methane and ethane emissions to the atmosphere from central and western U.S. oil and natural gas production regions. *Journal of Geophysical Research: Atmospheres*, *123*, 7725–7740. https://doi.org/10.1029/2018JD028622

Received 7 MAR 2018
Accepted 20 JUN 2018
Accepted article online 2 JUL 2018
Published online 24 JUL 2018

Quantifying Methane and Ethane Emissions to the Atmosphere From Central and Western U.S. Oil and Natural Gas Production Regions

J. Peischl[1,2], S. J. Eilerman[1,2,3], J. A. Neuman[1,2], K. C. Aikin[1,2], J. de Gouw[1,4], J. B. Gilman[2], S. C. Herndon[5], R. Nadkarni[6], M. Trainer[2], C. Warneke[1,2], and T. B. Ryerson[2]

[1]Cooperative Institute for Research in Environmental Sciences, University of Colorado Boulder, Boulder, CO, USA, [2]Chemical Sciences Division, NOAA Earth System Research Laboratory, Boulder, CO, USA, [3]Now at Jupiter, Boulder, CO, USA, [4]Department of Chemistry and Biochemistry, University of Colorado Boulder, Boulder, CO, USA, [5]Aerodyne Research, Inc., Billerica, MA, USA, [6]Texas Commission on Environmental Quality, Austin, TX, USA

Abstract We present atmospheric measurements of methane (CH_4) and ethane (C_2H_6) taken aboard a National Oceanic and Atmospheric Administration WP-3D research aircraft in 2015 over oil- and natural gas-producing regions of the central and western United States. We calculate emission rates from the horizontal flux of CH_4 and C_2H_6 in the planetary boundary layer downwind of five of these oil- and gas-producing regions: the Bakken in North Dakota, the Barnett in Texas, the Denver Basin in Colorado, the Eagle Ford in Texas, and the Haynesville in Texas and Louisiana. In general, we find that the enhancement of C_2H_6 relative to CH_4 in the atmosphere is similar to their relative abundances in locally produced natural gas. For the Bakken and Barnett regions, both absolute CH_4 emissions and the percentage of produced natural gas emitted to the atmosphere are consistent with previous studies. The percentage of produced natural gas emitted to the atmosphere was lower than in previous studies in the Denver Basin and the Haynesville regions, which may be due to a decrease in drilling activity, an increase in emission controls, or some combination thereof. Finally, we provide the first estimates of basin-wide emissions from the Eagle Ford region using in situ airborne data and find C_2H_6 emissions to be greater than those from the Bakken region. Emissions from the Bakken and Eagle Ford regions combined account for 20% of anthropogenic C_2H_6 emissions in North America.

1. Introduction

In March 2015, U.S. production of natural gas reached a then-record monthly high of 7.6×10^{10} m^3 (2.8 trillion cf, www.eia.gov), while U.S. crude oil production reached levels not seen since 1972. These totals represented a 40% increase in production since March 2006, due largely to the advancement of horizontal-drilling and hydraulic-fracturing techniques. Oil and natural gas (O&NG) production operations emit natural gas to the atmosphere both as a result of routine operations, such as through venting and the use of pneumatic controls, and unintentionally, via leaks and other fugitive emissions. Methane (CH_4) is typically the largest component of natural gas and is also a greenhouse gas (GHG) 28–34 times more potent than carbon dioxide on a 100-year time scale (Myhre et al., 2013). In the 2015 U.S. Environmental Protection Agency (EPA) GHG inventory (U.S. Environmental Protection Agency, 2017), emissions from O&NG production and processing accounted for 24% of human-caused CH_4 emissions in the United States. Additionally, unintended emissions of natural gas from the O&NG industry potentially represent an unknown loss of commodity.

In addition to CH_4, natural gas is a source of ethane (C_2H_6) and higher hydrocarbons to the atmosphere. C_2H_6 is typically the second-most abundant component of natural gas and is produced mainly via thermogenic processes. This makes it a useful tracer for fossil-based CH_4 emissions, especially in regions with significant microbial CH_4 sources, such as ruminants and landfills (Yacovitch et al., 2014) that complicate source identification from atmospheric CH_4 observations alone. Both CH_4 and C_2H_6 contribute to global background ozone production (e.g., Fiore et al., 2002; Tzompa-Sosa et al., 2017). Also, recent studies have used emissions of C_2H_6 as a tracer for the relative role that O&NG production has on the global CH_4 budget (e.g., Franco et al., 2016; Hausmann et al., 2016; Helmig et al., 2016; Schwietzke et al., 2014; Simpson et al., 2012). Global transport and chemistry models therefore need accurate O&NG CH_4 and C_2H_6 emission inventories in order to properly assess their impact on the global scale.

Numerous studies have examined CH_4 emissions from O&NG-producing regions in the United States in the past 10 years. These include top-down studies that quantify total CH_4 and C_2H_6 emissions using ambient measurements, bottom-up studies that quantify CH_4 emissions from individual components and processes, and studies to reconcile any differences between the two methods. Several top-down studies used measurements from aircraft to provide snapshots of emissions on a given day when meteorology is favorable for determining emissions; others were monthlong studies aimed at understanding the day-to-day variability of emissions. Here we use airborne in situ data to quantify emissions from regions studied previously using top-down methods: the Bakken shale region of North Dakota (Peischl et al., 2016), the Barnett shale region in Texas (Karion et al., 2015; Smith et al., 2015), the Denver Basin region (sometimes referred to as the Denver-Julesburg Basin or Wattenberg Field) in Colorado (Pétron et al., 2012, 2014), and the Haynesville shale region in Louisiana and Texas (Peischl et al., 2015). We also quantify emissions from a region not as well-studied, the Eagle Ford shale region in Texas. Emissions determined from one flight in the Upper Green River region in Wyoming will be discussed in a separate work.

Here we estimate total atmospheric CH_4 and C_2H_6 emissions from O&NG-producing regions using measurements made aboard a National Oceanic and Atmospheric Administration (NOAA) WP-3D (P-3) aircraft during March and April 2015 during the Shale Oil and Natural Gas Nexus (SONGNEX) field campaign. We then use a CH_4 emission inventory to estimate emissions from sources not related to the O&NG industry, such as livestock and landfills, and attribute the remaining CH_4 emissions to O&NG activity. We evaluate this attribution to O&NG sources by examining the enhancement ratio of C_2H_6 to CH_4 in the atmosphere downwind of the O&NG regions and comparing the enhancement to the abundance in natural gas from the region. We also examine the correlation of ammonia (NH_3) to CH_4 in the atmosphere to determine the impact livestock and manure management have on observed CH_4 enhancements. Next, we compare emissions from O&NG operations to production data in order to determine the percentage of produced natural gas that is emitted to the atmosphere. Finally, we compare our results to previously published work.

2. Instrumentation

During SONGNEX, the NOAA P-3 was equipped with 18 instruments measuring trace gases and particle microphysical properties. The specific measurements used for this analysis, along with their estimated uncertainties, are listed below.

2.1. CH_4

Methane was measured by wavelength-scanned cavity ringdown spectrometry (Picarro 1301-m, Sunnyvale, CA). Uncertainties were estimated by introducing standards near the inlet tip regularly throughout the project, as described by Peischl et al. (2012). The standards were calibrated to the World Meteorological Organization (WMO) scale (X2004A) before and after the project using a set of four standards calibrated by the NOAA Earth System Research Laboratory's Global Monitoring Division. A high and low standard were introduced in order to span the majority of ambient measurements, typically 2–4 times per flight, which we refer to as a "calibration." A third standard, or "target," was introduced 4–8 times per flight to check the stability and accuracy of the calibration by comparing its value retrieved in flight to that from the WMO scale. Over the course of SONGNEX, the retrieved value of this standard in flight was 1831.8 ± 0.6 ppb; the WMO standard value was 1831.6 ± 1.0 ppb. All uncertainties are reported herein as 1σ. For the CH_4 data reported here, we estimate a 1-Hz precision of ±0.4 ppb and a total uncertainty of ±1.2 ppb. All CH_4 data are reported as dry air mole fractions.

2.2. C_2H_6

Ethane was measured by tunable infrared laser direct absorption spectroscopy (Aerodyne mini ethane spectrometer, Billerica, MA; Yacovitch et al., 2014). Ultrapure zero air (Scott-Marrin Inc., Riverside, CA) and an C_2H_6 calibration standard (Matheson Linweld, Sioux City, IA) were regularly delivered to the inlet line to evaluate instrument sensitivity between approximately 0 and 100 ppbv C_2H_6 in flight. Instrument zeroes were determined in flight by sampling an excess of ultrapure zero air for 30 s approximately every 15 min and linearly interpolating the retrieved values; instrument calibrations were performed by standard replacement for 60 s approximately once every 2 hr in flight. These tanks were calibrated after the SONGNEX field project with a set of C_2H_6 standards obtained from the NOAA Earth System Research Laboratory's Global Monitoring

Division (Hall et al., 2007). Unlike the CH_4 measurement, the C_2H_6 sample was not dried. We estimate a 1-Hz precision of 0.04 ppbv and a total uncertainty of ±(0.07 ppbv + 2.1%) for C_2H_6 measurements. The uncertainty of the C_2H_6 measurement is reported as the following uncertainties added in quadrature: uncertainty of zero air, ±0.04 ppbv; uncertainty of interpolated zero, ±0.06 ppbv; C_2H_6 standard uncertainty, ±2% relative to the NOAA Earth System Research Laboratory GMD scale (Hall et al., 2007); and variability of in-flight standard retrieval, ±0.7%. C_2H_6 was also measured in whole air samples taken aboard the P-3 aircraft, and a comparison of the two measurements is presented by Lerner et al. (2017).

2.3. NH_3 and Meteorological Data

Ammonia was measured by chemical ionization mass spectrometry (Nowak et al., 2007). We estimate a 1-Hz precision of ±35 pptv and a total uncertainty of ±(25% + 500 pptv), determined from regular in-flight calibrations and instrument background checks. Meteorological and navigational measurements were made by various sensors aboard the NOAA P-3 and reported at 1 Hz. We estimate the following uncertainties for these measurements: wind speed (±1 m/s), wind direction (±5°), ambient temperature (±0.5 °C), potential temperature (θ, ±0.5 K), dew point temperature (±0.5 °C), heading (±0.5°), radar altitude (±15 m), GPS altitude (±16 m), H_2O (±5% in units of g/kg), and ground speed (±3.4 m/s). For comparisons of dry CH_4 fluxes to ambient C_2H_6 fluxes, H_2O corrections were less than 1% for all flights, with the exception of the two Eagle Ford flights, for which H_2O was ~2%. These corrections are either negligible or within the uncertainties of the emissions estimates stated below.

3. Additional Data

Well locations, O&NG production data, and natural gas composition data were obtained from various sources (e.g., Brandt et al., 2015; Hill et al., 2007; Rodriguez & Philp, 2010; Sherwood et al., 2017; see Text S1 in the supporting information). CH_4 emissions from sources not related to O&NG production, such as livestock and landfills, are derived from the work of Maasakkers et al. (2016), which partitioned the 2012 U.S. EPA CH_4 emissions inventory onto a 0.1° latitude × 0.1° longitude grid. We scale gridded enteric fermentation and manure management emissions by the ratio of the total number of cattle and calves for the counties in each region of interest in 2015 versus 2012. Cattle and calf data were downloaded from the U.S. Department of Agriculture National Agriculture Statistics Service website (https://www.nass.usda.gov). This scaling resulted in a change in estimated CH_4 emissions from enteric fermentation and manure management of $<$10% in each region. Emissions from individual grid cells are apportioned by geographic area in cases where the NOAA P-3 flight track intersected a grid cell. We assume a ±100% uncertainty in this inventory, in part because most of the non-O&NG sources are livestock-related, which have a 100% uncertainty at the 0.1° scale (Maasakkers et al., 2016). The U.S. EPA Greenhouse Gas Reporting Program (GHGRP) is used to locate CH_4 emissions from known point sources of CH_4 in 2015 (downloaded March 2017 from http://ghgdata.epa.gov/ghgp).

Accurate mass balance calculations of area source emissions require a spatially and temporally uniform wind field in order to satisfy the assumption that upwind emissions contribute with equal weighting to the enhancement above background of a measured gas downwind, because the enhancement scales with the inverse of the wind speed (Text S2). These wind measurements are made onboard the NOAA P-3, but the Hybrid Single-Particle Lagrangian Integrated Trajectory model (Stein et al., 2015), run with the North American Mesoscale 12-km resolution meteorological data and modeled vertical transport, is used to assess the spatial and temporal uniformity of wind fields before the arrival of the NOAA P-3 in a region.

We not only report volumes of natural gas in m^3 at 0 °C and 101.325 kPa and use this for our calculations but also provide the volumes in cubic feet (cf) and pressures in pounds per square inch (psi) as reported by the U.S. Energy Information Administration (EIA) or the states for reference. The following conditions are reported for natural gas volumes: EIA, Colorado, and North Dakota, 15.56 °C (60 °F) and 101.56 kPa (14.73 psi); Louisiana, 15.56 °C and 103.59 kPa (15.025 psi); and Texas, 15.56 °C and 101.01 kPa (14.65 psi).

4. Emission Flux Calculations

The mass balance technique (White et al., 1976) used here to quantify emissions has been extensively used to estimate CH_4 and C_2H_6 emissions from O&NG-producing regions in the United States, including the Uinta

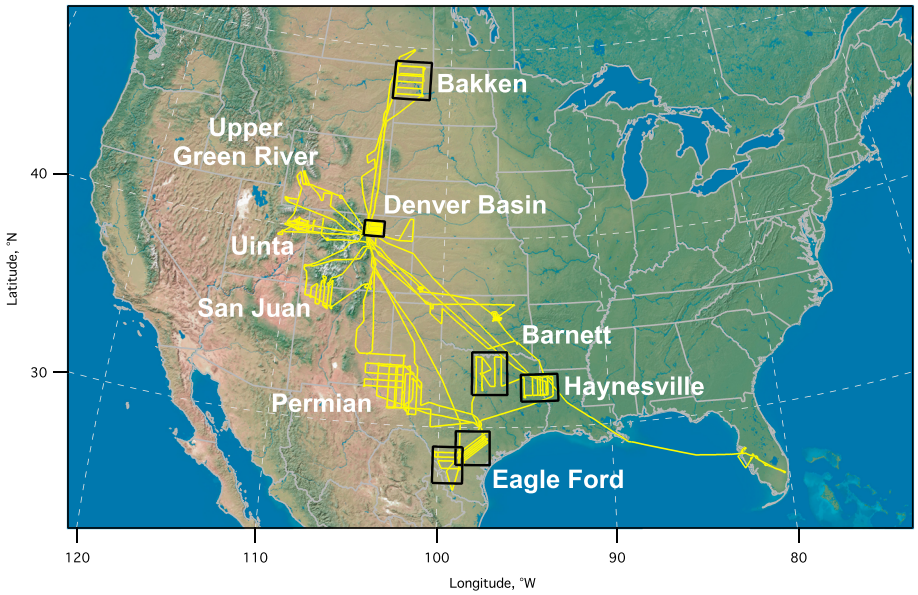

Figure 1. Map of central North America, with the National Oceanic and Atmospheric Administration P-3 flight tracks during the Shale Oil and Natural Gas Nexus field campaign shown as yellow lines. The black boxes represent the insets for the maps in Figures 2 and 3 and S1–S4.

Basin of Utah (Karion et al., 2013), the Denver Basin of northeastern Colorado (Pétron et al., 2014), the Marcellus shale region of northeastern Pennsylvania (Barkley et al., 2017; Peischl et al., 2015), the Fayetteville shale region of Arkansas (Peischl et al., 2015; Schwietzke et al., 2017), the Haynesville shale region of northwestern Louisiana and eastern Texas (Peischl et al., 2015), the Barnett shale region of Texas (Karion et al., 2015; Smith et al., 2015), the Bakken shale region of North Dakota (Kort et al., 2016; Peischl et al., 2016), and the San Juan region of New Mexico and Colorado (Smith et al., 2017). A similar mass balance technique has been used to quantify CH_4 and other emissions from portions of O&NG-producing regions and from large point sources (Caulton et al., 2014; Conley et al., 2016; Lavoie et al., 2017). The analysis and technique presented here expand upon the work of Peischl et al. (2015) and are summarized in Text S2.

5. Results

The SONGNEX field campaign comprised 18 flights of the chemically instrumented NOAA P-3 research aircraft in March and April 2015 upwind of, over, and downwind of regions with O&NG production in the central and western United States (Figure 1). Here we present airborne data from 5 regions: the Bakken shale in North Dakota; the Barnett shale near Dallas, Texas; the Denver Basin of northeastern Colorado; the Eagle Ford shale in southern Texas; and the Haynesville shale in eastern Texas/northwestern Louisiana. We quantify CH_4 and C_2H_6 emissions from these regions, compare these values to previous emission estimates, attribute CH_4 emissions specific to O&NG activity, and determine the amount of natural gas emitted to the atmosphere for each of these regions. To our knowledge, this work provides the first basin-wide estimate of atmospheric CH_4 and C_2H_6 emissions using airborne in situ data from the Eagle Ford region of Texas. Therefore, we use this region as an example below and present the analysis of the other regions in Text S3.

Figures 2 and 3 and S1–S4 show NOAA P-3 flight tracks colored by CH_4 mixing ratio in the boundary layer for each of the five O&NG-producing regions studied. The insets of the maps in these figures are represented by black rectangles in Figure 1. Data on reported O&NG production per well are gridded to highlight areas of the highest production in each region. The grid dimensions for a given region are roughly proportional to the area of the study region. Each grid is colored linearly such that white represents zero production, black represents the maximum production, and half the maximum gridded production is green for natural gas and cyan for oil.

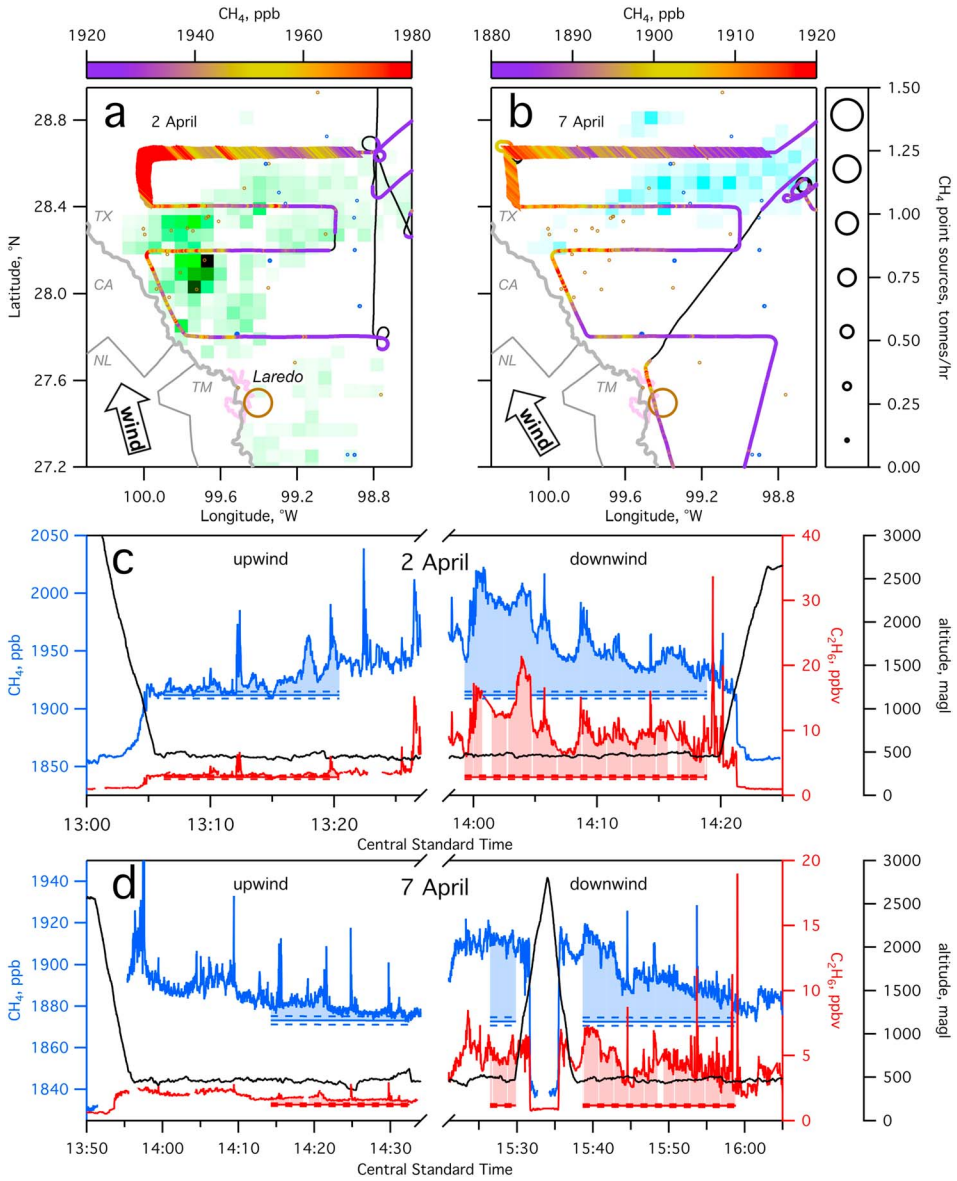

Figure 2. (a) Map of the western Eagle Ford study region, with the 2 April National Oceanic and Atmospheric Administration P-3 flight track represented by a thin black line colored by observed CH_4 in the boundary layer. The wider hash marks represent the downwind transect used for the mass balance calculation. Also shown is a 6.6 × 6.6 km grid of normalized natural gas production, where zero production is represented as white, the maximum production is represented as black, and the color scale is linearly interpolated through shades of green. Note: The maximum production grid is defined as the maximum for the entire Eagle Ford region, spanning Figures 5 and 6. CH_4 point sources are shown as open circles colored blue for oil- and gas-related sources and brown for all others, sized by emissions in the Environmental Protection Agency Greenhouse Gas Reporting Program inventory for 2015. (b) Map similar to (a), but for the 7 April flight. Normalized oil production is shown using cyan as the intermediate color. (c) Time series of CH_4 (blue), C_2H_6 (red), and altitude (black) from the 2 April flight. The enhancement used for the mass balance calculation is shaded above the estimated background. The dashed lines represent the background uncertainty. (d) A time series from the 7 April flight, with coloring and lines defined as in (c).

5.1. CH_4 and C_2H_6 Emissions

The NOAA P-3 sampled the Eagle Ford shale region of southern Texas on 2 and 7 April 2015 (Figures 2 and 3). We separate the region into two sections, west and east, due to the size of the region, the relative differences in O&NG production, and the different levels of background CH_4 upwind of the two regions. Figures 2 and 3 show reported O&NG production (section S1 in the supporting information) on a 6.6 × 6.6 km grid. In this case, the

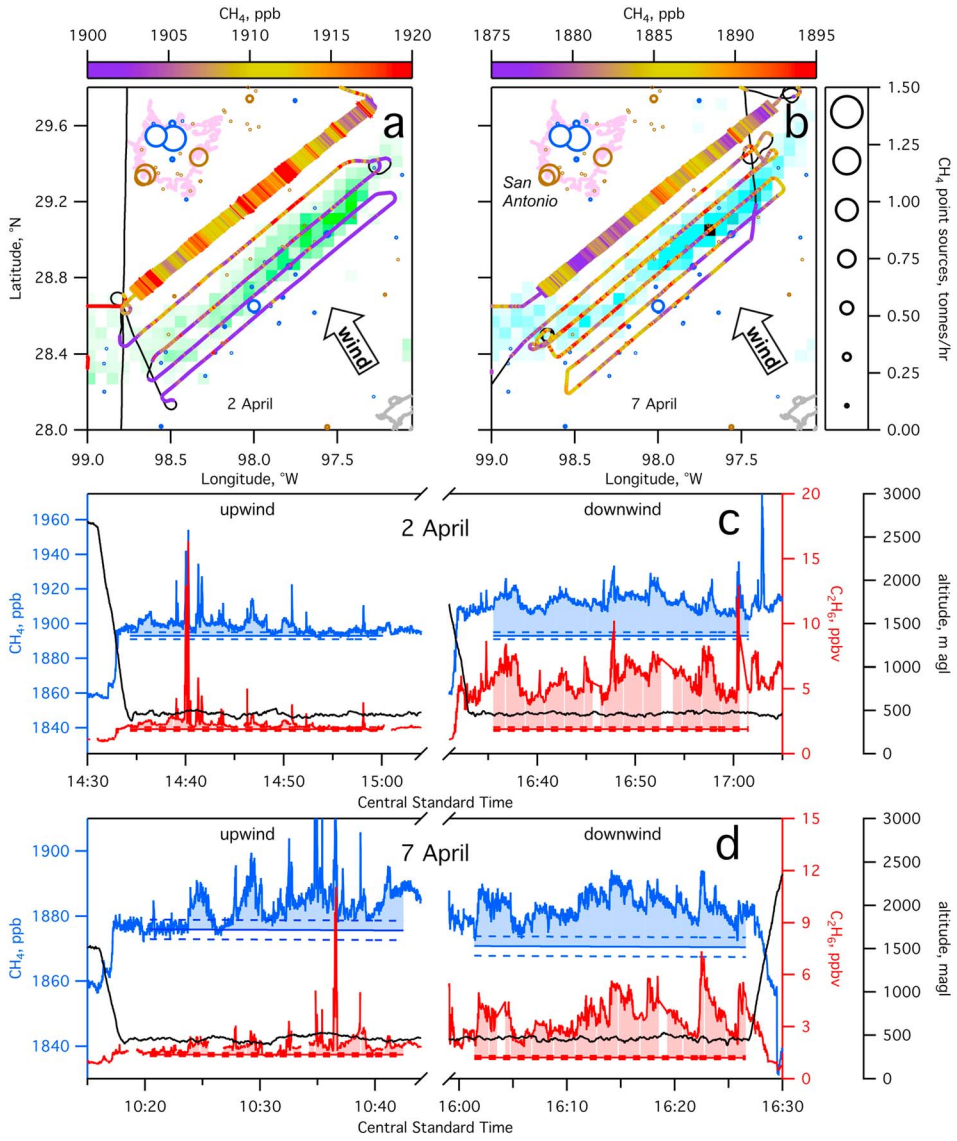

Figure 3. (a) Map of the eastern Eagle Ford study region, with the 2 April National Oceanic and Atmospheric Administration P-3 flight track represented by a thin black line colored by observed CH_4 in the boundary layer. The wider hash marks represent the downwind transect used for the mass balance calculation. Also shown is a 6.6 × 6.6 km grid of normalized natural gas production, where zero production is represented as white, the maximum production is represented as black, and the color scale is linearly interpolated through shades of green. Note: The maximum production grid is defined as the maximum for the entire Eagle Ford region, spanning Figures 5 and 6. CH_4 point sources are shown as open circles colored blue for oil- and gas-related sources and brown for all others, sized by emissions in the Environmental Protection Agency Greenhouse Gas Reporting Program inventory for 2015. Urban areas are outlined in pink; the large urban area in the northwestern part of the map is the San Antonio metropolitan area. (b) Map similar to (a), but for the 7 April flight. Normalized oil production is shown using cyan as the intermediate color. (c) Time series of CH_4 (blue), C_2H_6 (red), and altitude (black) from the 2 April flight. The enhancement used for the mass balance calculation is shaded above the estimated background. The dashed lines represent the background uncertainty. (d) A time series from the 7 April flight, with coloring and lines defined as in (c).

gridded production in Figures 2 and 3 is scaled to the maximum grid cell for the entire Eagle Ford region. The western region is where the majority of natural gas was produced, and the eastern region is where the majority of oil was produced in 2015. The P-3 flew further to the west on the 7 April flight than the 2 April flight and consequently sampled a factor of 1.07 more natural gas production. For our analysis, we take the weighted mean emission and compare it to a mean natural gas production upwind of the two flights (Table 1).

Table 1
Summary of C_2H_6 and CH_4 Emissions from Study Regions

Region	C_2H_6 emission (tonnes/hr)	CH_4 emission (tonnes/hr)	Estimated CH_4 emissions from O&NG activity (tonnes/hr)	Monthly NG production from emission region (10^9 m^3)	Abundance of CH_4 in natural gas (%)	NG produced emitted to atmosphere (%)
Bakken	27 ± 6	29 ± 7	28 ± 7	1.12 ± 0.02	47 ± 13	5.4 ± 2.0
Barnett	5.9 ± 2.0	66 ± 22	46 ± 30	3.64 ± 0.07	87 ± 3	1.5 ± 1.0
Denver Basin	7.0 ± 1.1	24 ± 5	18 ± 8	1.18 ± 0.02	77 ± 8	2.1 ± 0.9
Eagle Ford West	17 ± 3	42 ± 11	41 ± 11	2.7 ± 0.3	77 ± 10	2.0 ± 0.6
Eagle Ford East	20 ± 3	45 ± 10	42 ± 11	2.0 ± 0.2	68 ± 9	3.2 ± 1.1
Haynesville	4.5 ± 1.5	51 ± 16	42 ± 18	4.50 ± 0.23	90 ± 7	1.0 ± 0.5

5.1.1. Eagle Ford West

For the 2 April flight, winds were out of the south-southeast at 5.2 ± 1.0 m/s. We estimate the adjusted PBL depth to be 1,060 ± 250 m above ground level (agl) for the downwind transect following the method described in section S2; uncertainties in these two values constitute the majority of the uncertainty in the derived emission rates. We estimate the emission of CH_4 between the upwind transect at 27.8°N latitude and the downwind transect at 28.65°N (Figure 2) from the difference in CH_4 flux between the downwind and upwind transects (Peischl et al., 2015). Emissions from the largest point source in the 2015 GHGRP for the region, the City of Laredo Landfill located at 27.5°N and 99.4°W, scale to 1.2 tonnes CH_4/hr. This emission is accounted for by the upwind transect. We calculate a flux of CH_4 entering the region of 17 ± 7 tonnes CH_4/hr, shown as a light blue enhancement labeled "upwind" in Figure 2c. We subtract this from the flux exiting the region, shown as the light blue enhancement labeled "downwind" in Figure 2c, of 57 ± 14 tonnes CH_4/hr. The result is an emission from between the two transects of 41 ± 16 tonnes CH_4/hr. The terms do not sum to the total due to rounding. Similarly, we calculate an upwind flux of 1.1 ± 0.8 tonnes C_2H_6/hr and a downwind flux of 18 ± 6 tonnes C_2H_6/hr to determine an emission of 17 ± 7 tonnes C_2H_6/hr from the region. For the 7 April flight, winds were again out of the south-southeast at 8.1 ± 1.0 m/s. We estimate the adjusted PBL depth at 1,525 ± 230 m agl for the downwind transect. We calculate an emission of 44 ± 15 tonnes CH_4/hr and 17 ± 4 tonnes C_2H_6/hr. The largest sources of uncertainty were the wind speed, ±18%, and the boundary layer depth, ±15%. A $1/\sigma^2$-weighted average of the two flights results in emissions of 42 ± 11 tonnes CH_4/hr and 17 ± 3 tonnes C_2H_6/hr from the western Eagle Ford region (Table 1).

5.1.2. Eagle Ford East

For the 2 April flight, winds were out of the southeast at 7.3 ± 1.0 m/s. We estimate the adjusted PBL depth to be 1,220 ± 240 m agl for the downwind transect. We calculate an emission of 46 ± 12 tonnes CH_4/hr and 21 ± 6 tonnes C_2H_6/hr from the eastern portion of the Eagle Ford region. We estimate the uncertainty of interpolating the C_2H_6 measurement during zeroes to be ±18%. For the 7 April flight, winds were out of the southeast at 8.7 ± 1.7 m/s. We estimate the PBL depth to be 1,585 ± 240 m agl for the downwind transect. The estimated background mixing ratio has been adjusted linearly according to equation (S3) to account for dilution due to a growing PBL depth. The PBL depth grew by nearly a factor of 2 between the upwind transect and the downwind transect. We adjust the initial background estimate, 1,876 ppb, by accounting for dilution with approximately 1,860 ppb of CH_4 above the PBL (Figure 3d) and assign a ±3 ppb uncertainty to the background. We calculate an emission of 45 ± 21 tonnes CH_4/hr and 20 ± 4 tonnes C_2H_6/hr. We estimate the C_2H_6 interpolation uncertainty at ±18%. A weighted average of the two flights results in emissions of 45 ± 10 tonnes CH_4/hr and 20 ± 3 tonnes C_2H_6/hr (Table 1).

We perform a similar analysis for the other regions studied during SONGNEX (Text S3). We find emissions of 29 ± 7 tonnes CH_4/hr and 27 ± 6 tonnes C_2H_6/hr from the Bakken region, 66 ± 22 tonnes CH_4/hr and 5.9 ± 2.0 tonnes C_2H_6/hr from the Barnett region, 24 ± 5 tonnes CH_4/hr and 7.0 ± 1.1 tonnes C_2H_6/hr from the Denver Basin region, and 51 ± 16 tonnes CH_4/hr and 4.5 ± 1.5 tonnes C_2H_6/hr from the Haynesville region (Table 1).

5.2. Source Attribution

In this section, we estimate CH_4 emissions from sources related to O&NG production for the Eagle Ford region. Source attribution for the other regions is treated in Text S4. To accomplish this, we use a gridded 2012 U.S. EPA CH_4 inventory (Maasakkers et al., 2016) to estimate emissions *not* related to O&NG production in each region. These sources typically consist of enteric fermentation, manure management, landfills, wastewater treatment, and coal mining. We then check these estimates using airborne data. For example, we compare downwind atmospheric enhancements of C_2H_6 relative to CH_4 with natural gas composition data from the regions studied to see if produced natural gas emitted to the atmosphere could explain the enhancements and examine correlations of C_2H_6 and NH_3 with CH_4 under the assumption that co-emitted species will have higher a coefficient of determination (R^2).

5.2.1. Eagle Ford West

We estimate an emission of 0.9 tonnes CH_4/hr from the western portion of the Eagle Ford region not related to O&NG production and processing (Maasakkers et al., 2016). Enteric fermentation accounts for the majority of these emissions at 0.7 tonnes CH_4/hr.

Information on natural gas composition is sparse for the western Eagle Ford region. We therefore use composition data from a variety of generalized source analyses, with the C_2H_6:CH_4 ratio given for each reference: upstream of two gathering stations, 0.131 and 0.085 (Bowles, 2014); a sample from a transmission pipeline operator known to operate in the central and southern Eagle Ford region, 0.185 (George & Bowles, 2011); general Eagle Ford shale gas characteristics, 0.187 (Cohen, 2013) and 0.245 (Conder & Lawlor, 2014); and general Western Gulf Basin natural gas characteristics, 0.050 (Pring, 2012, Table E-2) and 0.094 (Lange et al., 2014, Table 4–2). Despite the limited natural gas composition data available for the western Eagle Ford region, the composition data generally bracket the atmospheric enhancements of C_2H_6 and CH_4 (Figure 4d). A linear least squares fit of the data from the downwind transect results in a slope of 0.116 and 0.080 ppbv C_2H_6/ppb CH_4 for the 2 and 7 April flights, respectively. The R^2 relationships on the 2 and 7 April flights were 0.19 and 0.00, respectively, for NH_3 and CH_4, and 0.73 and 0.54, respectively, for C_2H_6 and CH_4. Therefore, we conclude that O&NG activity is responsible for the majority of CH_4 emissions to the atmosphere in this region and attribute an emission of 41 ± 11 tonnes CH_4/hr from O&NG sources in the western Eagle Ford region out of a total emission of 42 ± 11 tonnes CH_4/hr (Table 1).

5.2.2. Eagle Ford East

We estimate an emission of 2.8 tonnes CH_4/hr from the eastern Eagle Ford region from sources not related to O&NG production and processing (Maasakkers et al., 2016). The majority of these emissions come from enteric fermentation, which accounts for 2.0 tonnes CH_4/hr.

Zhang et al. (2017) analyzed the chemical composition of natural gas from 37 Eagle Ford shale oil wells after hydraulic fracturing. The C_2H_6 and CH_4 composition of this gas is similar to the atmospheric enhancement of these compounds (Figure 4e). A linear least squares fit of the data from the downwind transect results in a slope of 0.185 and 0.205 ppbv C_2H_6/ppb CH_4 for the 2 and 7 April flights, respectively. Additionally, the R^2 relationships on the 2 and 7 April flights were 0.07 and 0.08, respectively, for NH_3 and CH_4, and 0.64 and 0.69, respectively, for C_2H_6 and CH_4. Therefore, we conclude that O&NG activity is again responsible for the majority of emissions in this region and attribute an emission of 42 ± 11 tonnes CH_4/hr from O&NG sources in the eastern Eagle Ford region out of a total emission of 45 ± 10 tonnes CH_4/hr (Table 1).

Similarly, we estimate CH_4 emissions from sources not related to O&NG operations of 1.1–1.4 tonnes CH_4/hr from the Bakken region, 20 tonnes CH_4/hr from the Barnett region, 5.9 tonnes CH_4/hr from the Denver Basin region, and 8.8 tonnes CH_4/hr from the Haynesville region (Text S4). These emissions are subtracted from the total emission to estimate a CH_4 emission from O&NG production in these regions (Table 1). Figure 4 shows that the atmospheric enhancements of C_2H_6 to CH_4 immediately downwind of O&NG-producing regions are similar to their abundance in natural gas from these regions. Additionally, in each region, the R^2 of C_2H_6 versus CH_4 is greater than for NH_3 versus CH_4, indicating that natural gas emissions are the larger source of CH_4 in these regions.

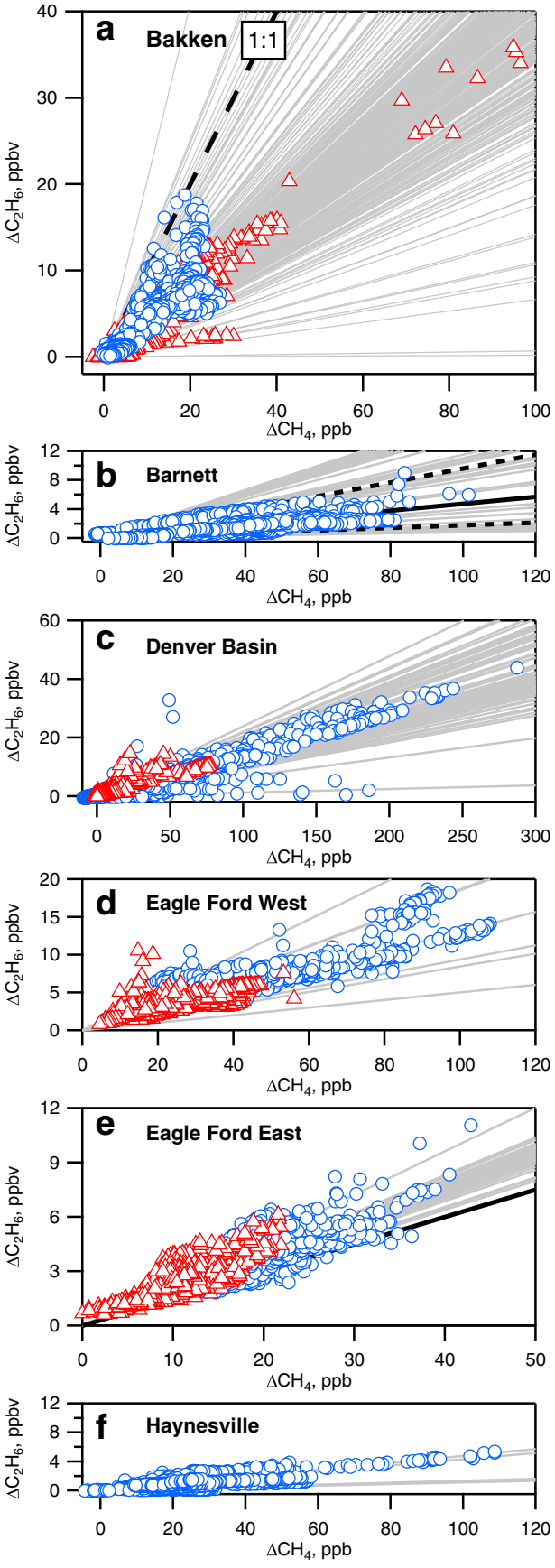

5.3. Natural Gas Production

Natural gas production is estimated using a combination of state and EIA data, where available. We first compare the totals derived from individual well production data to basin-wide totals to verify the well totals, then use high resolution well location data to estimate production upwind of the mass balance transects.

The EIA reports total Eagle Ford natural gas production in April 2015 at 5.91×10^9 m^3 (220 billion cf). Texas Railroad Commission county-level production estimates for April in the SONGNEX study region total 5.48×10^9 m^3, with 3.18×10^9 m^3 produced in the western counties (Dimmit, LaSalle, Maverick, and Webb), and 2.30×10^9 m^3 produced in the eastern counties (Atascosa, Bee, Dewitt, Gonzales, Karnes, Live Oak, McMullen, and Wilson). According to 2015 well production data from the Texas Railroad Commission, prorated natural gas production for the entire Eagle Ford region was only 3.14×10^9 m^3 (117 billion cf), which falls below the average statewide production reporting rate of 75%. For our calculations, we scale county-level production data by the well production locations with an estimated ±10% uncertainty. Natural gas production was $2.7 \pm 0.3 \times 10^9$ m^3 in the western Eagle Ford study region and $2.0 \pm 0.2 \times 10^9$ m^3 in the eastern Eagle Ford study region.

Natural gas production from the Bakken, Barnett, Denver Basin, and Haynesville regions is discussed in Text S5. We determine monthly natural gas production of $1.12 \pm 0.02 \times 10^9$ m^3 from the Bakken region, $3.64 \pm 0.07 \times 10^9$ m^3 from the Barnett region, $1.18 \pm 0.02 \times 10^9$ m^3 from the Denver Basin region, and $4.50 \pm 0.23 \times 10^9$ m^3 from the Haynesville region (Table 1).

5.4. Natural Gas Emissions to the Atmosphere

Here we calculate the volume of natural gas emitted to the atmosphere from O&NG operations and compare it to the volume of natural gas produced to derive the percentage of produced natural gas that is emitted to the atmosphere from each basin. We achieve this by taking the mass emission of CH_4 from O&NG operations in a region and converting it to a volume emission of natural gas based on the abundance of CH_4 in natural gas from a given region.

For the Eagle Ford region, there was a general lack of information on natural gas composition until the study by Zhang et al. (2017). A previous study of Eagle Ford emissions (Roest & Schade, 2017) relied on reports to the Texas Commission on Environmental Quality (Pring, 2012) to estimate the natural gas composition from this region. We use the results from Zhang et al. (2017) to represent eastern Eagle Ford natural gas

Figure 4. C_2H_6 to CH_4 enhancements above background from the downwind transects used in the mass balance calculation for each region (red and blue markers) are compared to the natural gas composition (gray lines) for the following regions: (a) Bakken, (b) Barnett, (c) Denver Basin, (d) western Eagle Ford, (e) eastern Eagle Ford, and (f) Haynesville. The dashed black line in (a) represents the 1:1 line. The aspect ratio is the same for each graph, so a direct comparison of slopes may be made. The solid black line in (b) represents the composition ratio used by Zavala-Araiza et al. (2014); the two dotted black lines in represent the highest frequency enhancement ratios reported by Smith et al. (2015). The black line in panel (e) represents the C_2H_6 to CH_4 ratio used by Roest and Schade (2017) to estimate CH_4 emissions from C_2H_6 measurements taken in the region.

composition, and the multiple studies cited in section 5.2, which includes the study by Pring (2012), to represent western Eagle Ford natural gas composition.

5.4.1. Eagle Ford West

Here we use the same studies that reported C_2H_6 and CH_4 abundance in natural gas for the source attribution to estimate CH_4 abundance in natural gas from the western Eagle Ford region. Bowles (2014) reports CH_4 abundances of 80.0% and 74.6% upstream of two natural gas processing plants in 2014, with a range between 74.5% and 88.7% between 2010 and 2014. George and Bowles (2011) report a CH_4 abundance of 74.6% from a pipeline operator in the region. Other reported general Eagle Ford/Western Gulf abundances include 75% (Cohen, 2013), 66.6% (Conder & Lawlor, 2014), 90.1% (Pring, 2012), and 77.15% (Lange et al., 2014). Based on these studies, we estimate a CH_4 abundance in natural gas from this region of 77 ± 10%, which results in 2.0 ± 0.6% of the natural gas produced in the region that is emitted to the atmosphere (Table 1).

5.4.2. Eagle Ford East

The mean abundance of CH_4 in 37 natural gas samples from oil wells by Zhang et al. (2017) taken from the eastern Eagle Ford region is 62 ± 3%. The atmospheric enhancements of C_2H_6 to CH_4 seem to be well represented by the composition from the Zhang et al. (2017) analyses, although there are likely emissions from the natural gas wells too. According to Texas Railroad Commission county production data, gas and oil wells produced an equal amount of natural gas in April 2015. Thus, our estimate of CH_4 abundance in natural gas from this region should include some portion of natural gas similar to that in the western Eagle Ford. We therefore estimate the abundance to be 68 ± 9% for the eastern Eagle Ford region, which covers the range of variability in the CH_4 abundance from oil wells and the mean abundance used for the western Eagle Ford region. This results in 3.2 ± 1.1% of the natural gas produced in the region that is emitted to the atmosphere (Table 1).

The abundance of CH_4 in natural gas from the Bakken, Barnett, Denver Basin, and Haynesville regions is determined from previous studies and reported in Text S6 and in Table 1. The resulting emissions of produced natural gas to the atmosphere are 5.4 ± 2.0% from the Bakken region, 1.5 ± 1.0% from the Barnett region, 2.1 ± 0.9% from the Denver Basin region, and 1.0 ± 0.5% from the Haynesville region.

6. Discussion

Here we compare the results of our analysis, specifically the estimated CH_4 and C_2H_6 emissions from O&NG activity and the percentage of produced natural gas emitted to the atmosphere, with previous work. To help frame a comparison of these numbers, we additionally present changes in the natural gas production and the drill rig count in these regions between studies. The drill rig count may be interpreted as a proxy for well completions, which are one of the larger sources of CH_4 during the O&NG drilling stages (U.S. Environmental Protection Agency, 2017).

6.1. Bakken

The CH_4 and C_2H_6 emissions attributed to O&NG operations in the Bakken region remained constant within uncertainties between May 2014 and April 2015. Peischl et al. (2016) attributed 26.5 ± 6.5 tonnes CH_4/hr to O&NG operations in May 2014, compared to 28 ± 7 tonnes CH_4/hr in April 2015. Similarly, Kort et al. (2016) reported emissions of 26 ± 8 tonnes C_2H_6/hr in May 2014, compared to 27 ± 6 tonnes C_2H_6/hr in this study. However, the natural gas produced in the region increased by a factor of 1.13 between these two studies in 2014 and 2015, which accounts for the small but not statistically significant decrease in the percentage of produced natural gas emitted to the atmosphere from 6.3 ± 2.1% to 5.4 ± 2.0%. Other factors may have contributed to a decrease in the percentage emitted as well, including the rig count, which decreased from 180 in May 2014 to 86 in April 2015. Additionally, Gvakharia et al. (2017) reported that up to one fifth of CH_4 emissions in the region could be accounted for from the incomplete combustion of flared natural gas. According to the State of North Dakota Industrial Commission, the volume of flared natural gas decreased by 20% between May 2014 and April 2015.

6.2. Barnett

The CH_4 and C_2H_6 emissions attributed to O&NG operations in the Barnett region also remained constant within reported uncertainties between March/October 2013 and April 2015. Karion et al. (2015) attributed

60 ± 11 tonnes CH_4/hr to O&NG operations in March/October 2013, compared to 46 ± 30 tonnes CH_4/hr attributed in this study for April 2015. Smith et al. (2015) reported an emission of 6.6 ± 0.2 tonnes C_2H_6/hr in March/October 2013, compared to 5.9 ± 2.0 tonnes C_2H_6/hr for this study. The estimates of the percentage of produced natural gas emitted to the atmosphere have remained nearly unchanged, 1.6 ± 0.3% versus 1.5 ± 1.0%, despite a decrease in the number of drill rigs from an average of 35 in March 2013, to 33 in October 2013, and finally to 6 in April 2015.

6.3. Denver Basin

The CH_4 and C_2H_6 emissions attributed to O&NG operations in the Denver Basin region also remained statistically unchanged between 2008 and March 2015. Pétron et al. (2012) attributed approximately 14.8 tonnes CH_4/hr, with a range of 8.2–28.8 tonnes CH_4/hr, to O&NG operations in the summer of 2008, compared to the 19.3 ± 6.9 tonnes CH_4/hr attributed by Pétron et al. (2014) in May 2012, and the 18 ± 8 tonnes CH_4/hr attributed by this study for March 2015. Our estimated percentage of produced natural gas emitted to the atmosphere of 2.1 ± 0.9% in the Denver Basin region in March 2015 is lower than the 4.0% (range of 2.3–7.7%) and 4.1 ± 1.5% emissions estimated by Pétron et al. (2012) and Pétron et al. (2014) for the Denver Basin during the summer of 2008 and May 2012, respectively. A Welch's *t* test comparing the percentage emitted reported here to that of Pétron et al. (2014) results in a *t* statistic of 1.7, which means there is roughly an 83% likelihood that the percentage of produced natural gas emitted to the atmosphere has decreased between the two studies. Future studies will be necessary to determine if this trend is significant.

Natural gas production increased by a factor of 1.7 between the 2012 study by Pétron et al. (2014) and this work in 2015. However, the drill rig count for the Denver Basin decreased from 45 in May 2012 to 30 in March 2015. In addition, the state of Colorado introduced new regulations to limit CH_4 and volatile organic compound emissions in the intervening years. Therefore, it is possible that the decrease in the percentage of produced natural gas emitted to the atmosphere is due to a decrease in the amount of drilling activity, an increase in effective regulation and/or emissions control, or a combination of these factors.

Robertson et al. (2017) used CH_4 measurements from mobile laboratories in 2014 to derive a median percentage of produced natural gas emitted from well pads in the Denver Basin of 2.1% (1.6–3.0%, 1-sigma range), which is nearly identical to our basin-wide estimate for March 2015. This implies that well pad emissions may be the dominant source of CH_4 emissions in this region. This is supported by the GHGRP inventory for point sources, which account for only 0.4 tonnes CH_4/hr from O&NG point sources, or approximately 2% of emissions attributed to O&NG operations.

Townsend-Small et al. (2016) estimated that roughly half of CH_4 emissions in the Denver Basin O&NG production region were due to biogenic sources of CH_4. Our estimates of the contribution from these sources, derived from the 2012 EPA GHG inventory (Maasakkers et al., 2016), account for one-quarter of the total CH_4 emission, which is half that of the Townsend-Small et al. (2016) estimate, but similar to the estimate by Pétron et al. (2014). Further, Eilerman et al. (2016) found that emission ratios of NH_3 to CH_4 derived from mobile laboratory measurements at the fence-line downwind of feedlots in this region were consistent with ratios of inventory emissions. We therefore assume that the Maasakkers et al. (2016) inventory of CH_4 emissions from biogenic sources is accurate.

6.4. Eagle Ford

The region-wide CH_4 and C_2H_6 emissions attributed to O&NG operations in the Eagle Ford region are the first basin-wide estimates derived using in situ airborne data, to our knowledge. Schneising et al. (2014) used satellite measurements between the periods 2006–2008 and 2009–2011 to determine an increase in CH_4 emissions from this area of 530 ± 330 Gg CH_4/yr, which scales to 61 ± 38 tonnes CH_4/hr. This is consistent with the combined emissions we report from the eastern and western Eagle Ford regions of 82 ± 16 tonnes CH_4/hr from O&NG operations. However, the estimate by Schneising et al. (2014) implies an atmospheric emission of roughly 12 ± 8% of the natural gas produced (Howarth, 2015), whereas our western and eastern Eagle Ford estimates were 2.0 ± 0.6% and 3.2 ± 1.1%, respectively. The number of drill rigs in the Eagle Ford region increased from 46 in January 2009 to 239 in December 2011, with an average of 112 during the time period Schneising et al. (2014) examined, and by April 2015 there were

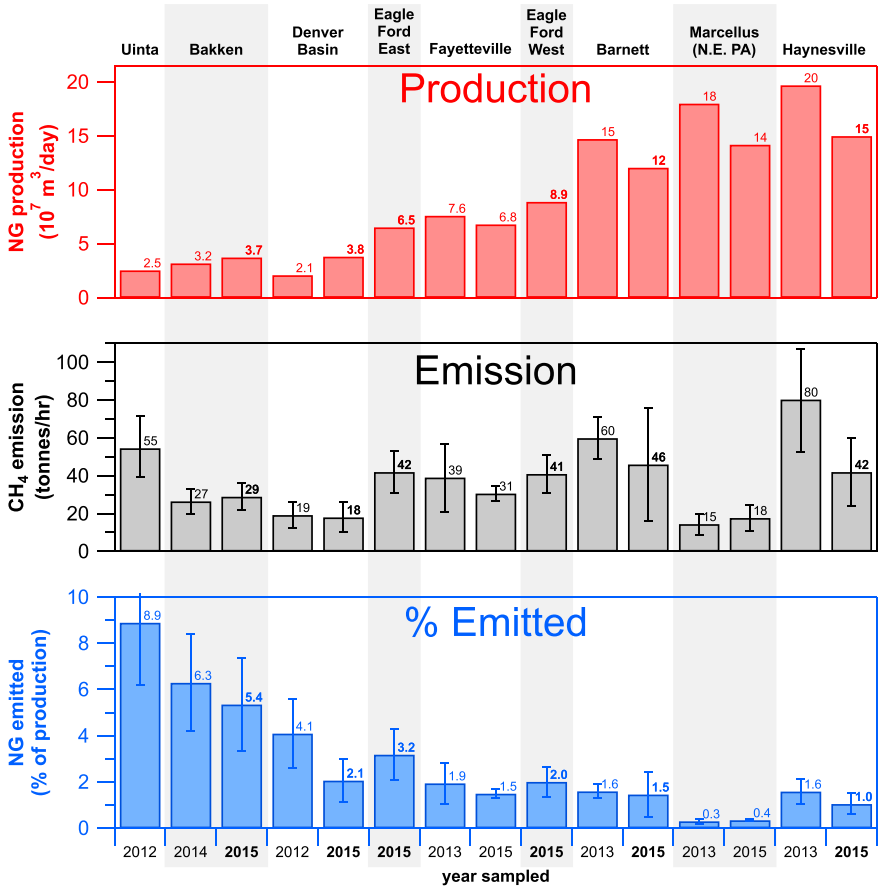

Figure 5. Summary of natural gas (NG) production, CH_4 emissions from oil and gas activity, and NG emitted as a percentage of natural gas produced in their respective regions. Numbers in boldface represent estimates presented in this study. Data from past studies are shown for comparison purposes (Barkley et al., 2017; Karion et al., 2013; Karion et al., 2015; Peischl et al., 2015; Peischl et al., 2016; Pétron et al., 2014; Schwietzke et al., 2017).

118 rigs in the region. The amount of drilling activity during our study was likely similar to the average drilling activity during the study by Schneising et al. (2014), which would not explain the differences in the percentage of produced natural gas emitted to the atmosphere.

Lavoie et al. (2017) used CH_4 measurements from small aircraft in June 2014 to determine emissions from large point sources in the eastern Eagle Ford region. They found aggregate emissions from large sources as a percentage of natural gas produced of 0.9 ± 0.3% and 1.3 ± 0.5% from their two study regions, which combine to average 1.1 ± 0.4%. Roest and Schade (2017) used ground-based measurements of C_2H_6 and other alkanes to derive an emission from upwind sources in the eastern Eagle Ford region of 0.7–1.6% (interquartile range) between August 2013 and August 2015. Our estimates of atmospheric emissions for the eastern Eagle Ford, 3.2 ± 1.1%, are significantly higher than these studies. One reason for this is our estimate of CH_4 and C_2H_6 abundance in produced natural gas from the region, which was determined from a study (Zhang et al., 2017) published after the studies by Lavoie et al. (2017) and Roest and Schade (2017) were published. Lavoie et al. (2017) calculated their emissions assuming produced natural gas was 100% CH_4. If they had instead used our estimated abundance, 68%, their combined average percentage of produced natural gas emitted to the atmosphere would have been 1.6 ± 0.6%, which is still lower than, but within the combined uncertainties of, our estimate. Roest and Schade (2017) used light alkane data from various sources to estimate the composition of raw natural gas and condensate tank gas from the region and then used the relative enhancements of light alkanes to attribute CH_4 emissions to raw natural gas and condensate tank emissions. It is therefore difficult to estimate how the inclusion of the data from Zhang et al. (2017) would affect their analysis.

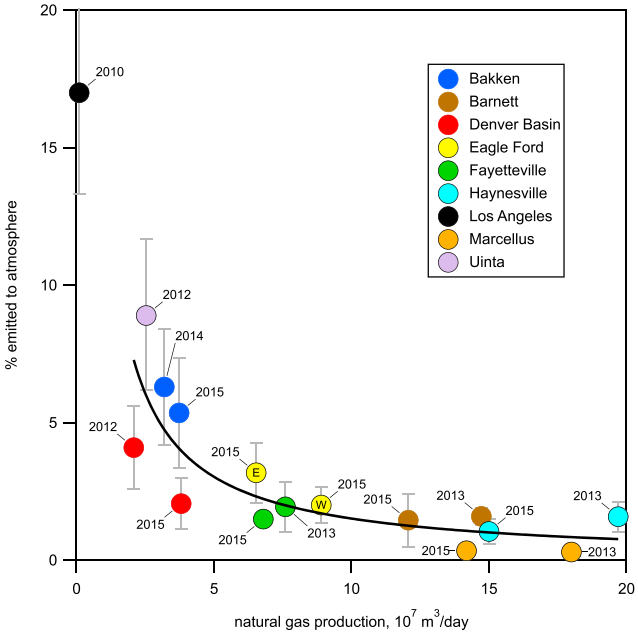

Figure 6. The percentage of produced natural gas emitted to the atmosphere is plotted against natural gas production. The eastern and western Eagle Ford emissions are represented by "E" and "W," respectively. The inverse relationship is expected, because production is the denominator of the percentage. A fit of a/x to the data in Figure 5, shown by the black line, represents a fixed emission versus varying production. Emissions from Los Angeles are included for comparison.

6.5. Haynesville

The CH_4 emissions attributed to O&NG operations in the Haynesville region have decreased in accordance with a decrease in natural gas production and drilling activity between June 2013 and April 2015. Natural gas production decreased from 6.0×10^9 m^3 in June 2013 to 4.5×10^9 m^3 in April 2015, drill rig count decreased from 43 to 32, estimated CH_4 emissions from O&NG activity decreased from 74 ± 28 tonnes CH_4/hr to 42 ± 18 tonnes CH_4/hr, and the percentage of produced natural gas emitted to the atmosphere decreased from 1.5 ± 0.5% to 1.0 ± 0.5%. The change in the percentage of natural gas lost is partly due to an increase in estimated emissions from sources unrelated to O&NG operations, from 6 tonnes CH_4/hr in 2013 to 9 tonnes CH_4/hr in 2015.

6.6. Additional Discussion

Figure 5 shows the results of Table 1 in graphical form. Also shown are previous airborne mass balance studies that reported total and percentage emissions for comparison. Regions are ordered by ascending natural gas production at the time they were last studied. We plot the percentage of produced natural gas emitted against production for each of the regions studied to better understand the relationship between changing emissions and production over time (Figure 6). An inverse relationship is expected because production is the denominator of the percentage of produced natural gas emitted. Therefore, an a/x fit to the data is shown with a black line. Emissions from Los Angeles (Peischl et al., 2013) were not used in the fit but are included for comparison. We use the Haynesville emission from 2015 to illustrate what this fit means, since the fit runs through this data point. The fit represents what the percentage of produced natural gas emitted to the atmosphere would be for a fixed Haynesville emission, 42 tonnes CH_4/hr in this case, at various Haynesville production rates. Therefore, if the percentage of produced natural gas emitted from a region were to move right along this curve, it would represent an increase in production with emission remaining constant, similar to what has happened in the Bakken and Denver Basin regions. Likewise, decreasing emissions with production remaining constant would result in the percentage of produced natural gas emitted moving downward on the graph. Although production decreased between the two studies of the Fayetteville and Haynesville regions, the percentages also moved downward on the graph. For the regions with multiple emission determinations, the percentages of produced natural gas emitted to the atmosphere have moved downward on the graph, suggesting more efficient production.

Recent work has noted the exceptionally large emission of C_2H_6 from the Bakken region of North Dakota (Helmig et al., 2016; Kort et al., 2016). Here we again find a similar emission of C_2H_6 from the Bakken region and an even larger total emission of C_2H_6 from the Eagle Ford region. If extrapolated to a yearly emission, the combined C_2H_6 emission from the Eagle Ford and Bakken regions, 64 ± 7 tonnes C_2H_6/hr, would account for 20% of North American anthropogenic emissions in 2014 estimated by Franco et al. (2016). We further note that C_2H_6-to-CH_4 emission ratios vary widely between basins, complicating budgets of O&NG CH_4 in the United States based on an assumed fixed relationship with C_2H_6.

Finally, although the NOAA P-3 sampled in the Uinta Basin in Utah, the San Juan Basin in New Mexico and Colorado, and the Permian Basin in Texas and New Mexico (Koss et al., 2017) during SONGNEX, we do not report emissions estimates from those regions due to variable winds that were less conducive to an accurate mass balance analysis. However, these flights may still be used to constrain emissions using inverse modeling techniques, but these studies will need to accurately account for the complex atmospheric transport on these days.

7. Conclusions

We calculate emissions of CH_4 and C_2H_6 from five oil- and natural gas-producing regions of the central and western United States: the Bakken region of North Dakota, the Barnett region of Texas, the Denver Basin region of Colorado, the Eagle Ford region of Texas, and the Haynesville region of Texas and Louisiana. To our knowledge, this is the first basin-wide estimate of emissions from the Eagle Ford region calculated using in situ airborne data.

We find emissions of natural gas to the atmosphere, in terms of the percentage of natural gas produced, ranging from 1.0 ± 0.5% in the Haynesville region of Texas and Louisiana to 5.4 ± 2.0% in the Bakken region of North Dakota. Our estimates of basin-wide natural gas emissions from the Denver Basin region are nearly identical to emissions in these regions determined from plume measurements from individual well pads by mobile laboratories (Robertson et al., 2017). This similarity might imply that well pad emissions account for the bulk of CH_4 emissions in this region.

Our estimate of C_2H_6 emissions from the Bakken region, 27 ± 6 tonnes C_2H_6/hr, is similar to that found by Kort et al. (2016), 27 ± 4 tonnes C_2H_6/hr. At the time, these emissions were noted because they were large enough to have played a significant role in the increasing background C_2H_6 at remote sites around the globe. Here we find an even larger emission from the Eagle Ford region of Texas of 37 ± 4 tonnes C_2H_6/hr. Combined, the Eagle Ford and Bakken regions account for 20% of anthropogenic C_2H_6 emissions in North America if extrapolated to a yearly emission (Franco et al., 2016).

In cases where we revisited oil- and natural gas-producing regions, we generally found that the percentage of natural gas produced emitted to the atmosphere decreased compared to previous studies. This may be a function of decreased natural gas production, decreased drilling activity, increased emission control or regulation, or some combination of these factors. Further study will be necessary to assess the statistical significance of these trends.

Acknowledgments
Data from the NOAA P-3 SONGNEX campaign are available to the public at https://esrl.noaa.gov/csd/groups/csd7/measurements/2015songnex/P3/DataDownload/. J.d.G. worked as a consultant for Aerodyne Research, Inc. during the preparation phase of this manuscript. The authors report no conflicts of interest.

References

Barkley, Z. R., Lauvaux, T., Davis, K. J., Deng, A., Miles, N. L., Richardson, S. J., et al. (2017). Quantifying methane emissions from natural gas production in north-eastern Pennsylvania. *Atmospheric Chemistry and Physics*, *17*(22), 13,941–13,966. https://doi.org/10.5194/acp-17-13941-2017.

Bowles, E. Jr. (2014). Effect of shale plays on U.S. natural gas composition. *Pipeline & Gas Journal*, *241*(7), 38–41.

Brandt, A. R., Yeskoo, T., McNally, S., Vafi, K., Cai, H., & Wang, M. Q. (2015). Energy intensity and greenhouse gas emissions from crude oil production in the Bakken formation: Input data and analysis methods, Department of Energy, Argonne National Laboratory. Retrieved from https://greet.es.anl.gov/publication-bakken-oil

Caulton, D. R., Shepson, P. B., Santoro, R. L., Sparks, J. P., Howarth, R. W., Ingraffea, A. R., et al. (2014). Toward a better understanding and quantification of methane emissions from shale gas development. *Proceedings of the National Academy of Sciences*, *111*(17), 6237–6242. https://doi.org/10.1073/pnas.1316546111

Cohen, A. K. (2013). The Shale Gas Paradox: Assessing the impacts of the shale gas revolution on electricity markets and climate change (bachelor of arts thesis). Retrieved from https://www.hks.harvard.edu/centers/mrcbg/publications/awp/awp14. Cambridge, MA: Harvard University.

Conder, M. W., & Lawlor, K. A. (2014). Production characteristics of liquids-rich resource plays challenge facility design, The American Oil & Gas Reporter, http://www.aogr.com/magazine/sneak-peek-preview/production-characteristics-of-liquids-rich-resource-plays-facility-design.

Conley, S., Franco, G., Faloona, I., Blake, D. R., Peischl, J., & Ryerson, T. B. (2016). Methane emissions from the 2015 Aliso Canyon blowout in Los Angeles, CA. *Science*, *351*, 1317–1320. https://doi.org/10.1126/science.aaf2348(6279)

Eilerman, S. J., Peischl, J., Neuman, J. A., Ryerson, T. B., Aikin, K. A., Holloway, M. W., et al. (2016). Characterization of ammonia, methane, and nitrous oxide emissions from concentrated animal feeding operations in northeastern Colorado. *Environmental Science & Technology*, *50*(20), 10,885–10,893. https://doi.org/10.1021/acs.est.6b02851

Fiore, A. M., Jacob, D. M., Field, B. D., Streets, D. G., Fernandes, S. D., & Jang, C. (2002). Linking ozone pollution and climate change: The case for controlling methane. *Geophysical Research Letters*, *29*(19), 1919. https://doi.org/10.1029/2002GL015601

Franco, B., Maheiu, E., Emmons, L. K., Tzompa-Sosa, Z. A., Fischer, E. V., Sudo, K., et al. (2016). Evaluating ethane and methane emissions associated with the development of oil and natural gas extraction in North America. *Environmental Research Letters*, *11*(4), 044010. https://doi.org/10.1088/1748-9326/11/4/044010

George, D. L., & Bowles, E. B. Jr. (2011). Shale gas measurement and associated issues. *Pipeline & Gas Journal*, *238*(7), 38–41.

Gvakharia, A., Kort, E. A., Brandt, A., Peischl, J., Ryerson, T. B., Schwarz, J. P., et al. (2017). Methane, black carbon, and ethane emissions from natural gas flares in the Bakken shale, North Dakota. *Environmental Science & Technology*, *51*(9), 5317–5325. https://doi.org/10.1021/acs.est.6b05183

Hall, B., Dutton, G. S., & Elkins, J. W. (2007). The NOAA nitrous oxide standard scale for atmospheric observations. *Journal of Geophysical Research*, *112*, D09305. https://doi.org/10.1029/2006JD007954

Hausmann, P., Sussmann, R., & Smale, D. (2016). Contribution of oil and natural gas production to renewed increase in atmospheric methane (2007–2014): Top-down estimate from ethane and methane column observations. *Atmospheric Chemistry and Physics*, *16*(5), 3227–3244. https://doi.org/10.5194/acp-16-3227-2016

Helmig, D., Rossabi, S., Hueber, J., Tans, P., Montzka, S. A., Masarie, K., et al. (2016). Reversal of global atmospheric ethane and propane trends largely due to US oil and natural gas production. *Nature Geoscience*, *9*(7), 490–495. https://doi.org/10.1038/ngeo2721

Hill, R. J., Jarvie, D. M., Zumberge, J., Henry, M., & Pollastro, R. M. (2007). Oil and gas geochemistry and petroleum systems of the Fort Worth Basin. *AAPG Bulletin*, *91*(4), 445–473. https://doi.org/10.1306/11030606014

Howarth, R. W. (2015). Methane emissions and climatic warming risk from hydraulic fracturing and shale gas development: Implications for policy. *Energy and Emission Control Technologies*, *3*, 45–54. https://doi.org/10.2147/EECT.S61539

Karion, A., Sweeney, C., Kort, E. A., Shepson, P. B., Brewer, A., Cambaliza, M., et al. (2015). Aircraft-based estimate of total methane emissions from the Barnett shale region. *Environmental Science & Technology*, *49*(13), 8124–8131. https://doi.org/10.1021/acs.est.5b00217

Karion, A., Sweeney, C., Pétron, G., Frost, G., Hardesty, R. M., Kofler, J., et al. (2013). Methane emissions estimate from airborne measurements over a western United States natural gas field. *Geophysical Research Letters*, *40*, 4393–4397. https://doi.org/10.1002/grl.50811

Kort, E. A., Smith, M. L., Murray, L. T., Gvakharia, A., Brandt, A. R., Peischl, J., et al. (2016). Fugitive emissions from the Bakken shale illustrate the role of shale production in global ethane shift. *Geophysical Research Letters*, *43*, 4617–4623. https://doi.org/10.1002/2016GL068703

Koss, A., Yuan, B., Warneke, C., Gilman, J. B., Lerner, B. M., Veres, P. R., et al. (2017). Observations of VOC emissions and photochemical products over US oil- and gas-producing regions using high-resolution H_3O^+ CIMS (PTR-ToF-MS). *Atmospheric Measurement Techniques*, *10*(8), 2941–2968. https://doi.org/10.5194/amt-10-2941-2017

Lange, B., Pring, M., & Treimel, S. (2014). Specified oil & gas well activities emissions inventory update ERG no. 0292.03.026.001. Retrieved from https://www.tceq.texas.gov/assets/public/implementation/air/am/contracts/reports/ei/5821199776FY1426-20140801-erg-oil_gas_ei_update.pdf. Morrisville, NC: Eastern Research Group, Inc.

Lavoie, T. N., Shepson, P. B., Cambaliza, M. O. L., Stirm, B. H., Conley, S., Mehrotra, S., et al. (2017). Spatiotemporal variability of methane emissions at oil and natural gas operations in the Eagle Ford Basin. *Environmental Science & Technology*, *51*(14), 8001–8009. https://doi.org/10.1021/acs.est.7b00814

Lerner, B. M., Gilman, J. B., Aikin, K. C., Atlas, E. L., Goldan, P. D., Graus, M., et al. (2017). An improved, automated whole-air sampler and gas chromatography mass spectrometry analysis system for volatile organic compounds in the atmosphere. *Atmospheric Measurement Techniques*, *10*(1), 291–313. https://doi.org/10.5194/amt-10-291-2017

Maasakkers, J. D., Jacob, D. J., Sulprizio, M. P., Turner, A. J., Weitz, M., Wirth, T., et al. (2016). Gridded national inventory of U.S. methane emissions. *Environmental Science & Technology*, *50*(23), 13,123–13,133. https://doi.org/10.1021/acs.est.6b02878

Myhre, G., Shindell, D., Bréon, F.-M., Collins, W., Fuglestvedt, J., Huang, J., et al. (2013). Anthropogenic and natural radiative forcing. In T. F. Stocker, et al. (Eds.), *Climate change 2013: The physical science basis*, *Contribution of Working Group I to the Fifth Assessment Report of the Intergovernmental Panel on Climate Change*, (pp. 659–740). Cambridge, United Kingdom and New York, NY: Cambridge University Press.

Nowak, J. B., Neuman, J. A., Kozai, K., Huey, L. G., Tanner, D. J., Holloway, J. S., et al. (2007). A chemical ionization mass spectrometry technique for airborne measurements of ammonia. *Journal of Geophysical Research*, *112*, D10S02. https://doi.org/10.1029/2006JD007589

Peischl, J., Karion, A., Sweeney, C., Kort, E. A., Smith, M. L., Brandt, A. R., et al. (2016). Quantifying atmospheric methane emissions from oil and natural gas production in the Bakken shale region of North Dakota. *Journal of Geophysical Research: Atmospheres*, *121*, 6101–6111. https://doi.org/10.1002/2015JD024631

Peischl, J., Ryerson, T. B., Aikin, K. C., de Gouw, J. A., Gilman, J. B., Holloway, J. S., et al. (2015). Quantifying atmospheric methane emissions from the Haynesville, Fayetteville, and northeastern Marcellus shale gas production regions. *Journal of Geophysical Research: Atmospheres*, *120*, 2119–2139. https://doi.org/10.1002/2014JD022697

Peischl, J., Ryerson, T. B., Brioude, J., Aikin, K. C., Andrews, A. E., Atlas, E., et al. (2013). Quantifying sources of methane using light alkanes in the Los Angeles basin, California. *Journal of Geophysical Research: Atmospheres*, *118*, 4974–4990. https://doi.org/10.1002/jgrd.50413

Peischl, J., Ryerson, T. B., Holloway, J. S., Trainer, M., Andrews, A. E., Atlas, E. L., et al. (2012). Airborne observations of methane emissions from rice cultivation in the Sacramento Valley of California. *Journal of Geophysical Research*, *117*, D00V25. https://doi.org/10.1029/2012JD017994

Pétron, G., Frost, G., Miller, B. R., Hirsch, A. I., Montzka, S. A., Karion, A., et al. (2012). Hydrocarbon emissions characterization in the Colorado Front Range: A pilot study. *Journal of Geophysical Research*, *117*, D04304. https://doi.org/10.1029/2011JD016360

Pétron, G., Karion, A., Sweeney, C., Miller, B. R., Montzka, S. A., Frost, G. J., et al. (2014). A new look at methane and nonmethane hydrocarbon emissions from oil and natural gas operations in the Colorado Denver-Julesburg Basin. *Journal of Geophysical Research: Atmospheres*, *119*, 6836–6852. https://doi.org/10.1002/2013JD021272

Pring, M. (2012). Condensate tank oil and gas activities. ERG no. 0292.01.011.001. Retrieved from https://www.tceq.texas.gov/assets/public/implementation/air/sip/hgb/RS_Report_Attachment_C.pdf. Morrisville, NC: Eastern Research Group, Inc.

Robertson, A. M., Edie, R., Snare, D., Soltis, J., Field, R. A., Burkhart, M. D., et al. (2017). Variation in methane emission rates from well pads in four oil and gas basins with contrasting production volumes and compositions. *Environmental Science & Technology*, *51*(15), 8832–8840. https://doi.org/10.1021/acs.est.7b00571

Rodriguez, N. D., & Philp, R. P. (2010). Geochemical characterization of gases from the Mississippian Barnett shale, Forth Worth Basin, Texas. *AAPG Bulletin*, *94*(11), 1641–1656. https://doi.org/10.1306/04061009119

Roest, G., & Schade, G. (2017). Quantifying alkane emissions in the Eagle Ford shale using boundary layer enhancement. *Atmospheric Chemistry and Physics*, *17*(18), 11,163–11,176. https://doi.org/10.5194/acp-17-11163-2017

Schneising, O., Burrows, J. P., Dickerson, R. R., Buchwitz, M., Reuter, M., & Bovensmann, H. (2014). Remote sensing of fugitive methane emissions from oil and gas production in North American tight geologic formations. *Earth's Future*, *2*, 548–558. https://doi.org/10.1002/2014EF000265(10)

Schwietzke, S., Griffin, W. M., Matthews, H. S., & Bruhwiler, L. M. P. (2014). Natural gas fugitive emissions rates constrained by global atmospheric methane and ethane. *Environmental Science & Technology*, *48*(14), 7714–7722. https://doi.org/10.1021/es501204c.

Schwietzke, S., Pétron, G., Conley, S., Pickering, C., Mielke-Maday, I., Dlugokencky, E. J., et al. (2017). Improved mechanistic understanding of natural gas methane emissions from spatially resolved aircraft measurements. *Environmental Science & Technology*, *51*(12), 7286–7294. https://doi.org/10.1021/acs.est.7b01810

Sherwood, O. A., Schwietzke, S., Arline, V. A., & Etiope, G. (2017). Global inventory of gas geochemistry data from fossil fuel, microbial and burning sources, version 2017. *Earth System Science Data*, *9*(2), 639–656. https://doi.org/10.5194/essd-9-639-2017

Simpson, I. J., Andersen, M. P. S., Meinardi, S., Bruhwiler, L., Blake, N. J., Helmig, D., et al. (2012). Long-term decline of global atmospheric ethane concentrations and implications for methane. *Nature*, *488*(7412), 490–494. https://doi.org/10.1038/nature11342

Smith, M. L., Gvakharia, A., Kort, E. A., Sweeney, C., Conley, S. A., Faloona, I., et al. (2017). Airborne quantification of methane emissions over the four corners region. *Environmental Science & Technology*, *51*(10), 5832–5837. https://doi.org/10.1021/acs.est.6b06107

Smith, M. L., Kort, E. A., Karion, A., Sweeney, C., Herndon, S. C., & Yacovitch, T. I. (2015). Airborne ethane observations in the Barnett shale: Quantification of ethane flux and attribution of methane emissions. *Environmental Science & Technology*, *49*(13), 8158–8166. https://doi.org/10.1021/acs.est.5b00219

Stein, A. F., Draxler, R. R., Rolph, G. D., Stunder, B. J. B., Cohen, M. D., & Ngan, F. (2015). NOAA's HYSPLIT atmospheric transport and dispersion modeling system. *Bulletin of the American Meteorological Society*, *96*(12), 2059–2077. https://doi.org/10.1175/BAMS-D-14-00110.1

Townsend-Small, A., Botner, E. C., Jimenez, K. L., Schroeder, J. R., Blake, N. J., Meinardi, S., et al. (2016). Using stable isotopes of hydrogen to quantify biogenic and thermogenic atmospheric methane sources: A case study from the Colorado front range. *Geophysical Research Letters*, *43*, 11,462–11,471. https://doi.org/10.1002/2016GL071438

Tzompa-Sosa, Z. A., Mahieu, E., Franco, B., Keller, C. A., Turner, A. J., Helmig, D., et al. (2017). Revisiting global fossil fuel and biofuel emissions of ethane. *Journal of Geophysical Research: Atmospheres*, *122*, 2493–2512. https://doi.org/10.1002/2016JD025767

U.S. Environmental Protection Agency (2017). Inventory of U.S. greenhouse gas emissions and sinks: 1990–2015, report # EPA 430-P-17-001. Retrieved from https://www.epa.gov/ghgemissions/inventory-us-greenhouse-gas-emissions-and-sinks

White, W. H., Anderson, J. A., Blumenthal, D. L., Husar, R. B., Gillani, N. V., Husar, J. D., & Wilson, W. E. Jr. (1976). Formation and transport of secondary air pollutants: Ozone and aerosols in the St. Louis urban plume. *Science*, *194*(4261), 187–189. https://doi.org/10.1126/science.959846

Yacovitch, T. I., Herndon, S. C., Roscioli, J. R., Floerchinger, C., McGovern, R. M., Agnese, M., et al. (2014). Demonstration of an ethane spectrometer for methane source identification. *Environmental Science & Technology*, *48*(14), 8028–8034. https://doi.org/10.1021/es501475q

Zavala-Araiza, D., Sullivan, D. W., & Allen, D. T. (2014). Atmospheric hydrocarbon emissions and concentrations in the Barnett shale natural gas production region. *Environmental Science & Technology*, *48*(9), 5314–5321. https://doi.org/10.1021/es405770h

Zhang, T., Sun, X., Milliken, K. L., Ruppel, S. C., & Enriquez, D. (2017). Empirical relationship between gas composition and thermal maturity in Eagle Ford shale, South Texas. *AAPG Bulletin*, *101*(08), 1277–1307. https://doi.org/10.1306/09221615209